مجلة الدراسات التربوية والعلمية - كلية التربية - الجامعة العراقية
العدد الخامس والعشرون - المجلد الأول - علوم الفيزياء - آذار 2025 م
doi.org/10.52866/esj.2025.01.25.20

Calculate the X-ray intensity ratio ($K_{\beta1}/K_{\alpha1}$) of noble gas

Lubna H. Ismael
Department of Physics, College of Education for Pure Sciences, University of Mosul

Abstract:

The ATOMOPM program was used to determine the effective central potential of electrons in an atom using the variation principle. Following that, the reduced diagonal Schrödinger equation method was utilized to calculate the potential integral and determine the atomic potential of a single particle. The voltage rate is taken between repetitions till self-consistency to calculate potential, wave state, orbital eigenvalues, and total energy. The DIRACATOMOPM program was employed to numerically solve the Dirac equation and turn it into a Schrödinger equation on the assumption that the interaction between electrons is mediated by a Coulomb potential. Non-relativistic calculations were used to approximate the a priori guess and begin the iteration process of solving the integral equation related to the relative potential calculations with the numerical solution of the Dirac equation until reaching the self-consistent factor (SCF) to determine the effective mutual potential, wave state, and total energy. The goal was to determine ratio of the X-ray intensity of the two lines ($K_{\beta1}$, $K_{\alpha1}$) for the noble gases and determine the relationship between the wavelength of these lines and the atomic number as well as the relationship between the X-ray intensity and frequency. The frequency was calculated using the Moseley equation, and the wavelength and frequency of the X-ray intensity were determined. The results are in good agreement with the theoretical and available experimental results.

Keywords: Nobel gases, $K_{\beta1}/K_{\alpha1}$ ratio, x-ray Spectra.

حساب نسبة شدة الاشعة السينية ($K_{\beta1}/K_{\alpha1}$) للغازات الخاملة

لبنى حقي إسماعيل, جامعة الموصل, كلية التربية للعلوم الصرفة ,قسم الفيزياء

مستخلص:

استخدام برنامج (ATOMOPM) لتحديد الجهد المركزي الفعال للإلكترونات في الذرة باستخدام مبدأ التباين. بعد ذلك، تم استخدام طريقة معادلة شودنكر القطرية المخفضة لحساب التكامل المحتمل وتحديد الجهد الذري لجسيم المنفرد. يتم أخذ معدل الجهد بين التكرارات حتى الاتساق الذاتي لحساب الجهد ودالة الموجة والقيم الذاتية والطاقة الكلية. كذلك استخدام برنامج (DIRACATOMOPM) لحل معادلة ديراك عدديًا وتحويلها إلى معادلة شودنكر على افتراض أن التفاعل بين الإلكترونات يتم بوساطة جهد كولوم. كذلك تم استخدام الحسابات الغير النسبية لتقريب التخمين المسبق وبدء عملية التكرار لحل معادلة التكامل المتعلقة بحسابات الجهد النسبي مع الحل العددي لمعادلة ديراك حتى الوصول إلى عامل الاتساق الذاتي (SCF) لتحديد الجهد المتبادل الفعال وحالة الموجة والطاقة الكلية. وكان الهدف هو حساب نسبة شدة الأشعة السينية للخطين ($K_{\beta1}$، $K_{\alpha1}$) للغازات الخاملة وتحديد العلاقة بين الطول الموجي لهذه الخطوط والعدد الذري وكذلك العلاقة بين شدة الأشعة السينية والتردد. تم حساب التردد باستخدام معادلة موزلي، وتم حساب الطول الموجي وتردد شدة الأشعة السينية. نتائج البحث تتفق بشكل جيد مع النتائج النظرية والتجريبية المتوفرة.

الكلمات المفتاحية: نسبة الغازات الخاملة، $K_{\beta1}/K_{\alpha1}$ أطياف الاشعة السينية.

Introduction

In the X-ray analysis approaches, a beam with a specific energy hits the sample, producing main ionizations in several inner-shells of the atoms. In fact, de-excitation of the atom from the ionized state releases the characteristic x-ray line which is the fingerprint for investigation. The quantity of $K_\beta/K\alpha$ intensity ratios represents a key factor for comparison with numerical calculations focuses on the atomic models to exam the reliability of these models. The Kα x-ray arises from the *L* to the *K* shell transitions. Similarly, the K_β X ray arises from the *M*-, *N*-, O-, etc., to the *K*-shell transitions [1]. Furthermore, significant theoretical estimations depended on the relativistic Hartree –Fock and Hartree–Slater models calculated by Scofield [2,3]. Who reported a study on the probability of the radioactive transition K_β, K_α of 26-elements of low atomic numbers Na_{11} to Rh_{45} in crystalline and non-crystalline systems. they compared the results with the previous results based on the efforts of Relativistic Hartree–Fock (RHFS) and relativistic Coulomb shielding potentials by Salem.. et al [4]. *K* shell x-ray fluorescence cross-sections were measured for some elements by Durak and Özdemir et al [6 ,7]. The results of the present work will be compared with previous empirical results achieved by different approaches, theoretical calculations, and semi-empirical calculations described in the previous studies. To the best of our knowledge, the *K*-shell fluorescence yields using a fluorescence excitation method were measured for the first time for Cs, Eu, and Hg by Durak ..et al [8]. $K_\beta/K\alpha$ and K X-ray fluorescence cross sections and $K_\beta/K\alpha$ intensity ratios of 17 metals from Cr to Bi were studied. The targets were irradiated with 59.5 and 123.6 keV photons from ^{241}Am and ^{57}Co sources. The results were associated with experimental and theoretical calculations reported by Cevik..et al [10]. Moreover, the x-ray cross-sections and the intensity ratios for Cr, Mn, Fe, and Co exposed by 8.735 keV photon source by means of secondary-excitation technique was studied by Yılmaz [11].The study of Ka and Kb x-ray cross-sections and the Kb=Ka x-ray intensity ratios for several targets in the range of$28) \leq Z \leq 39)$ irradiated by 16.896 keV photons using

secondary-excitation technique was reported by Yılmaz [12]. In this study, the (DIRAC ATOMOPM) software was used to solve the Dirac equation numerically for the Coulomb potential in order to study the role of the energy of the single particle as well as its effect on the relativistic wave function. In this regard, the intensity of the x-rays of the $K_{\beta 1}$, $K_{\alpha 1}$ lines of noble gases was calculated. The numerical outcomes in this study compared with both the experiments and calculations results in literatures. It is found that there is a good agreement between both experimental and numerical results in literatures.

Background and theory

An empty state in the *K* shell of the atom could be occupied by an electron from higher shells through radioactive transition, and x-ray photon may be emitted. The $K_{\beta 1}$ and $K_{\alpha 1}$ lines results when *K* shell empty state is occupied by an electron from M_3 and L_3 subshells, respectively. The intensity ratio of these lines can be given by the following equation15]].

$$I_{k\beta 1} \Big/ I_{k\beta 1} = \left(\frac{E_{k\alpha 1}}{E_{k\beta 1}}\right)^3 \left(\frac{Z-\sigma_L}{Z-\sigma_M}\right)^3 \left(\frac{n_M}{n_L}\right)^3 \text{---------(1)}$$

Where E_x= (x=β1, α1) is the energies of the emitted *K* x-ray photos, n_x and Z_x (x= L, M) are the principal quantum number and the effective change, of the L and M shells, respectively. Thus, precise knowledge of the electronic binding energies is required. This can be accomplished by solving Schrodinger equation and use the results as a starting approximation for Dirac equation. This method includes solving the Dirac equation and converting it into an equation similar to the Schrodinger equation. The small component and it is expressed interest of the large component.

$$-\left[\frac{d}{dr}-\frac{K}{r}\right]h(r)\left[\frac{d}{dr}+\frac{K}{r}\right]g(r)+V(r)g(r)=\varepsilon g(r) \text{-------(2)}$$

were

$$h(r)=\left[1+\left[\varepsilon-V(r)\right]/c^2\right]^{-1} \text{-----(3)}$$

and V(r) represents the total potential.

$$y(r) = h(r)^{1/2}\, g(r) ----(4)$$

If g(r) is switched by ($y(r) = h(r)^{1/2} g(r)$ false), the radial equation can be written as;

$$-y''(r) + \frac{k(k+1)}{r^2} Y(r) + \frac{W(r)}{h(r)} Y(r) = \frac{\varepsilon}{h(r)} y(r) ----(5)$$

were

$$W(r) = V(r) + \frac{3}{4} h(r)^3 \left[\frac{V'(r)}{c^2}\right]^2 + \frac{1}{2} h(r)^2 \left[\frac{V''(r)}{c^2}\right] - h(r)^2 \left[\frac{V'(r)}{c^2}\right] \frac{k}{r} ---(6)$$

Numerov's Method is used to solve the differential equation (5) [13,14].

Results and discussion:

Six-noble gases from group VIII in periodic table were taken under consideration in this study. which were suggested as inert gasses until 1960s. This was owing to the value of their oxidation number is 0, which avoids the noble gasses to procedure compounds swiftly. All noble gases exhibited a maximum number of electrons possible in their outer shell (2 for Helium, and 8 for the others), making them stable elements. These neutral noble gas atoms are listed in table 1.

Table.1 Noble gas atoms with their atomic numbers

Noble gas atoms	Helium	Neon	Argon	Krypton	Xenon	Radon
Z	2	10	18	36	54	86

In this research, we used the (ATOMOPM) software as a Schrödinger and Dirac program. In addition, the DARAC ATOMON software, to calculate the Dirac equation numerically for the Coulomb potential - the assumption of calculating the ratio of the x-ray emission ($I_{K\beta 1}$ /$I_{k\alpha 1}$) for the elements of the carrier gases (Z=10, 18, 36, 54, and 86) where the wave state cannot be used. Except for the northern wave The Qatari non-ratio hydrogen revolution in the form of ($\sigma \sim (\alpha\, z/\, n)^{3/2}$) for the permitted electron transitions at ($\ell = 0$) can

be stated in the quantum statement (ϕ) by (Z-σ) where in the constant south and the Islamic sticks and assuming that the intensity of the dipole transition is proportional .With the energy cube of the X-ray photon as shown in the equation. [15]

$$I_{k\beta 1} \Big/ I_{k\beta 1} = \left(\frac{E_{k\alpha 1}}{E_{k\beta 1}}\right)^3 \left(\frac{Z-\sigma_L}{Z-\sigma_M}\right)^3 \left(\frac{n_M}{n_L}\right)^3$$

σ_L =3.5, σ_M =8.5, n_M=3 (M shell), n_L=2(L shell)

The results were arranged in Table 2and were compared with the calculations [16]. These results were also plotted in Figure 1. The energy of the X-ray photon for each of the two lines $K_{\alpha 1}$ and $K_{\beta 1}$ for the atomic number(Z). It was shown that x-ray photon energy for ($K_{\beta 1}$) line increases more than the of ($K_{\alpha 1}$) line when the atomic number increases.

Table.2 Calculated binding energies and observed binding energies from the compilation of Thompson et. al [16]

Atoms	Present Results $E_{\alpha'}$(Rydberg)	Reported Results $E_{\alpha'}$(Rydberg) [16]	Present Results $E_{\beta'}$ (Rydberg)	Reported Results $E_{\beta'}$(Rydberg) [16]
Neon	60.0232	62.364484		
Argon	212.30181	217.2136268	228.6767383	234.46400352
Krypton	916.41432	925.73591	1052.21929	1036.62489
Xenon	2155.72652	2164.85979	2452.95438	2466.56866
Radon	2155.72652	5958.39917	6928.81097	6936.97806

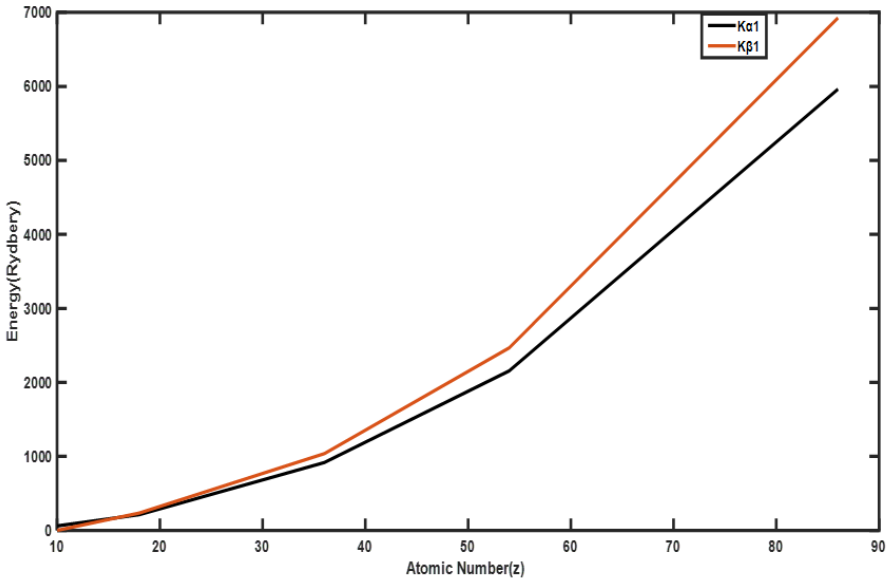

Fig.1 Energy Position of $K_{\alpha 1}$ and $K_{\beta 1}$ X-ray lines as a function of atomic number(Z)

As for Table. 3, it represents how the wavelength changes with the atomic number of the two $\lambda_{\alpha1}$ and $\lambda_{\beta1}$ lines if compared with the T calculations. The relationship between the wavelength of the $\lambda_{\beta1}$ lines and the atomic number was also drawn. We note that the wavelength of the $\lambda_{\beta1}$ line increases more than the wavelength of the $\lambda_{\alpha1}$ line as the atomic number Figure 2.

Table.3 Calculate the wavelength of the two lines of X-rays $\lambda_{\beta1}$ and $\lambda_{\alpha1}$ [16].

Atoms	Present Results λ_{α} (A)	Reported Results λ_{α} (A) [16]	Present Results λ_{β} (A)	Reported Results λ_{β} (A) [16]
Neon	0.05472	0.05683		
Argon	0.19375	0.197967	0.20841	0.213689
Krypton	0.83521	0.843715	0.93438	0.94477
Xenon	1.96472	1.973045	2.23561	2.24802
Radon	5.434780	5.619060	6.314891	6.31322

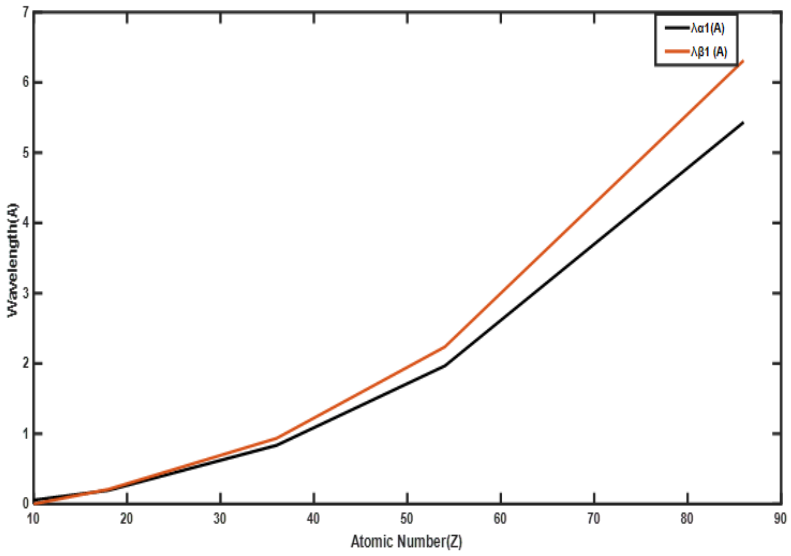

Fig.2 Wavelength of $\lambda_{\alpha1}$ and $\lambda_{\beta1}$ lines as a function of atomic number Z

As shown in Fig 3, we notice a relationship between the frequency square root of the of x-rays light against the atomic number. The square root of the frequency was found using Moseley's equation according to the following relationship.

$$(V)^{1/2} = A\,(Z - Z_0)$$

Where Z atomic number A and Z_0 are constants

Series K	where	$Z_0=1$	$A_\alpha=4.97x10^7$
Series L	where		$A_\alpha=2.14 * 10^7$ $Z_0=4.7$

It was found that the square root y frequency of the x-ray increases with increasing the atomic number.

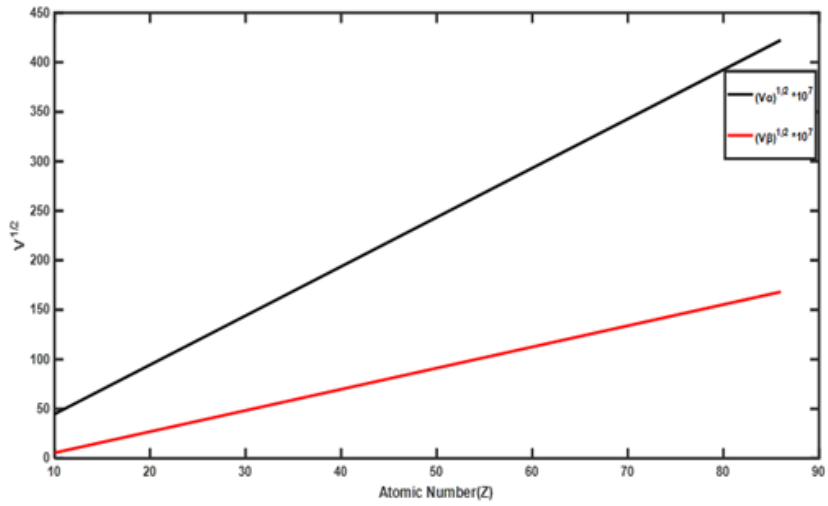

Fig.3 Frequency of $(V_{\alpha 1})^{1/2}$ and $(V_{\beta 1})^{1/2}$ lines versus atomic number

Fig. 4 and 5 they represent the relationship between the wavelength and the intensity of X-rays $E_{\alpha 1}$ and $E_{\beta 1}$ lines, where it is clear that the wavelength of the $\lambda_{\beta 1}$ line increases significantly more than the wavelength of the $\lambda_{\alpha 1}$ line.

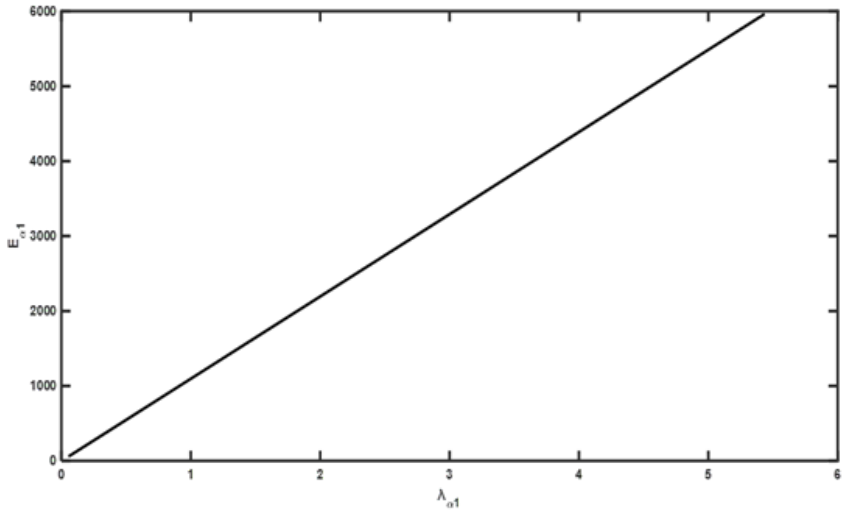

Fig. 4 The relationship between the wavelength and energy of the X-ray

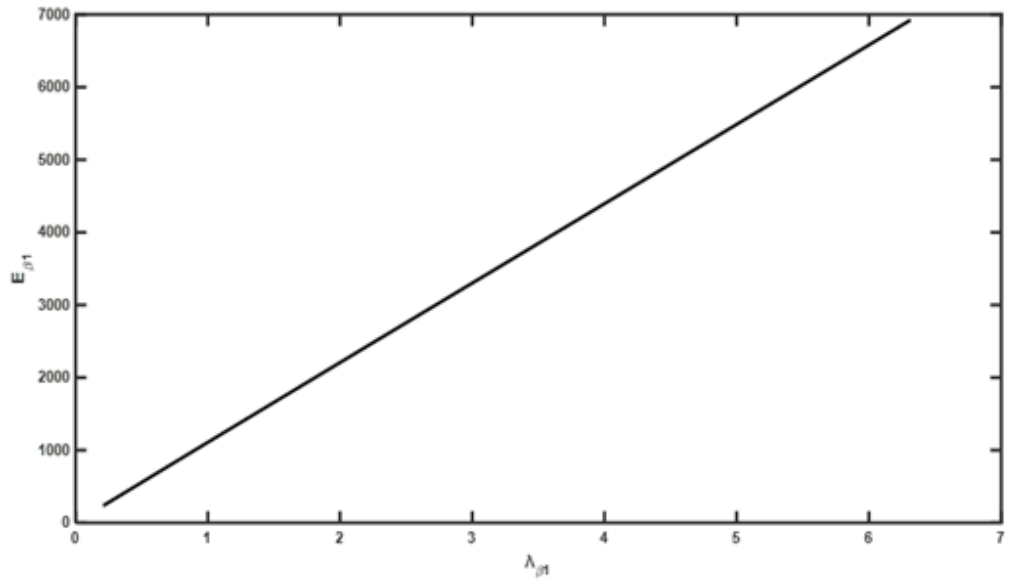

Fig.5 The relationship between the wavelength and energy of the X-ray

Figure 6-7 shows the relationship between the frequency emitted by the X-rays of the $V_{\alpha 1}^{1/2}$ line and the wavelength, where it was shown that the wavelength is inversely proportional to the frequency and the intensity of the x-rays.

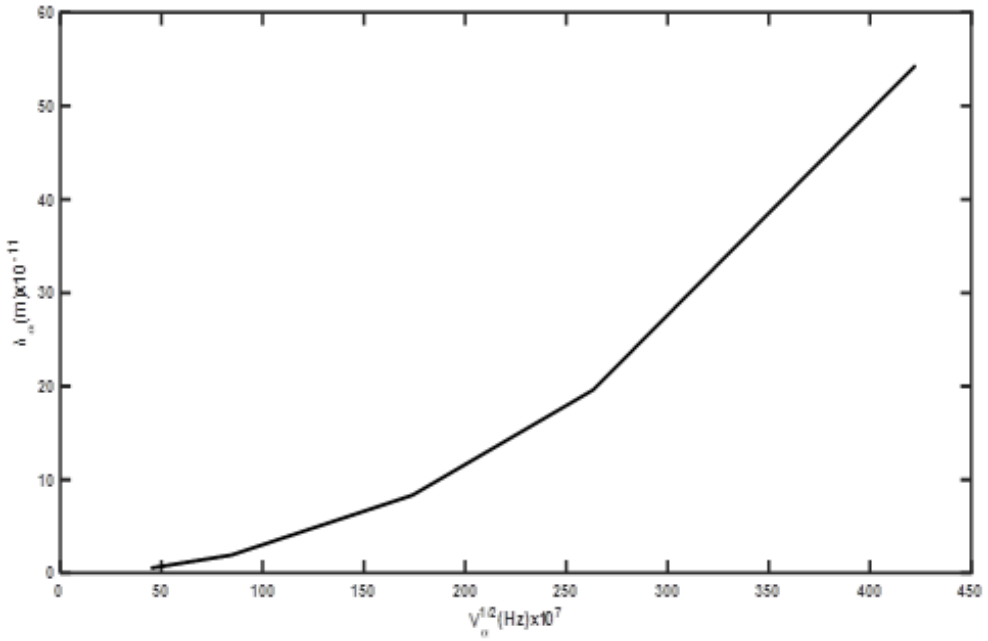

Fig. 6. Relationship between X-ray frequency and wavelength.

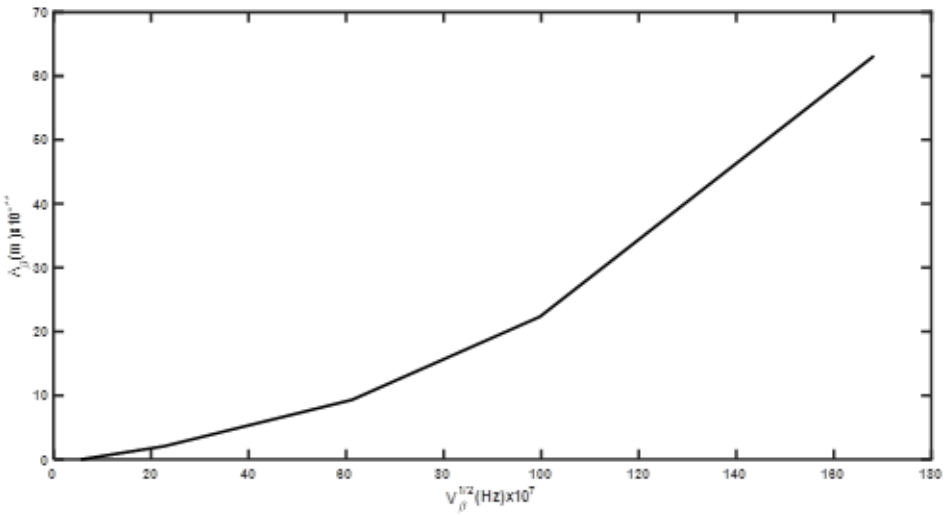

Fig.7 Relationship between X-ray frequency and wavelength

Figure 8 shows the relationship between the ratio of the intensity of the X-rays $E_{k\alpha2}/E_{k\alpha1}$ with the atomic number. It was compared with the experimental results [16], where it was shown that the ratio $E_{k\alpha2}/E_{k\alpha1}$ decreases with increasing atomic number. This means that the intensity of the line increases when the atomic number $E_{k\alpha2}$ is increased while the intensity of the $E_{k\alpha1}$ line decreases with increasing atomic number.

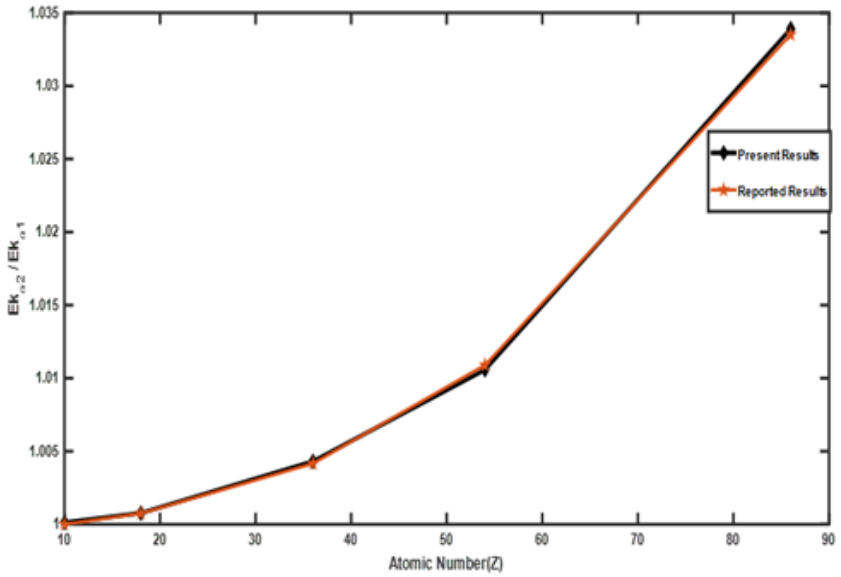

Fig.8. The $E_{k\alpha2}/E_{k\alpha1}$ radiative transition rate ratio versus atomic number.

X-ray intensity ratio ($I_{k\beta1}/I_{k\alpha1}$) was calculated as a function of the atomic number(Z). The results are arranged in Table 4, if they are compared with the calculations of [17,18], and also the experimental measurements findings of energy [16,18]. These results are also shown in Figure 9. indicates that the current calculations agree acceptably with the calculations of [16,18]. It is also clear from this table that the ratio ($I_{k\beta1}/I_{k\alpha1}$) decreases with increasing atomic number. This means that the intensity of the ($K_{\beta1}$) line rises when atomic number is increased while, the intensity of the ($K_{\alpha1}$) line drops when atomic number is increased, i.e. the probability of filling the empty in the K shell from the M_3 shell increases instead of filling it from the L_3 shell.

Table.4 Comparison between Present Results of the X-ray intensity ratio $I_{k\beta1}/I_{k\alpha1}$ and Reported Results. [16,17,18]

$I_{K\alpha1}/I_{K\beta1}$				
Z	Present Results	Reported Results [16]	Reported Results [17]	Reported Results [18]
Argon	9.587	9.521	9.54	9.428
Krypton	3.965	3.964	4.0	3.95
Xenon	3.109	3.100	3.200	3.106
Radon	2.584	2.584	2.525	2.587

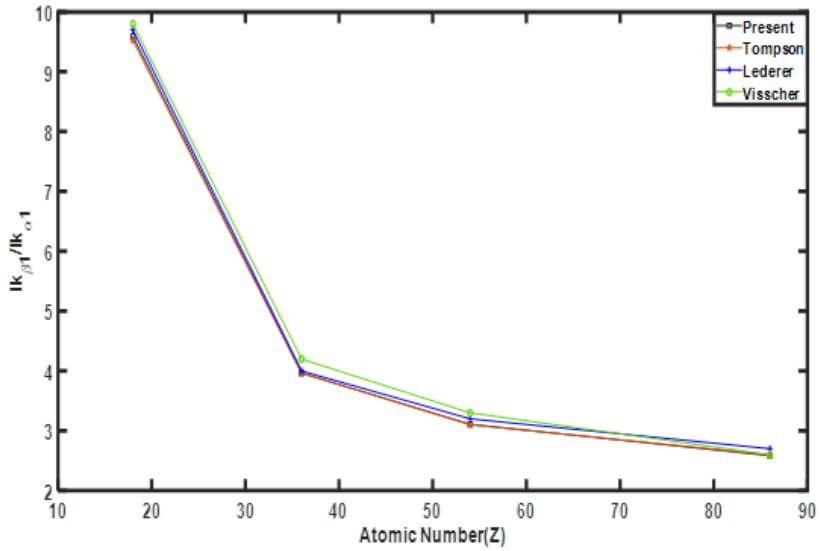

Fig.9 The present calculated K X-ray intensity ratio compared with relativistic (Dirac - Fock) and experimental results [17].

Conclusions:

The results obtained in the present work are in good agreement with other theoretical results and also with experimental data. This fast can be observed in tables (2,3,4). The Schrödinger equation was solved numerically for noble gases with atomic number (10, 18 ,36, 54 ,86) and the results were used as initial predictions for the relative state using the Coulomb potential. It was found that the energy of the photon energy of x-ray ($E_{\beta 1}$) line increases more than the photon energy of x-ray ($E_{\alpha 1}$) line as the atomic number increases and at the atomic setting of (86, 54). As for the wavelength of the line $\lambda_{\beta 1}$ it is greater than the wavelength of the line $\lambda_{\alpha 1}$ as the atomic number increases. The relationship between the frequency square root of x-ray light and the atomic number was observed. The results showed that the frequency increases with the increase in the atomic number. Moreover, the wavelength is subjected to the intensity of the x-ray photon energy of the two lines $K_{\alpha 1}$and $K_{\beta 1}$. The x-ray intensity ratio of the $E_{k\alpha 2}/E_{k\alpha 1}$ lines was recorded and showed an increase a with increasing atomic number. This means that the intensity of the $E_{k\alpha 2}$ line increases with increasing Z while the intensity of the $E_{k\alpha 1}$ line decreases. The ratio of the X-ray intensity of the two lines ($I_{k\beta 1}/I_{k\alpha 1}$) for noble gases was found with increasing atomic number with the ratio, which means the possibility of the electron moving from M_3 to K in order to fill the gap in K.

References

[1] M. Polasik, Theoretical multiconfiguration Dirac-Fock method study on the x-ray spectra of multiply ionized heavy atoms: The structure of the KaL M' lines, Phys. Rev. A. 40 (1989) 4361–4368.

[2] J.H. Scofield, Relativistic hartree-slater values for K and L X-ray emission rates, At. Data Nucl. Data Tables. 14 (1974) 121–137. https://doi.org/10.1016/S0092-640X(74)80019-7.

[3] J.H. Scofield, Exchange corrections of K x-ray emission rates, Phys. Rev. A. 9 (1974) 1041–1049. https://doi.org/10.1103/PhysRevA.9.1041.

[4] S.I. Salem, T.H. Falconer, Kp/Kcf Radiative-Transition-Probability Ratios for Elements of Low

Atomic Numbers in Amorphous and Crystal Forms, Phys. L RE VIE W A. 6 (1972).

[5] A. Küçükönder, E. Büyükkasap, R. Yilmaz, Y. Şahin, Chemical Effects on the K β /K α Intensity Ratios in First-Row Transition Element Compounds , Acta Phys. Pol. A. 95 (1999) 243–250. https://doi.org/10.12693/aphyspola.95.243.

[6] Y. Özdemir, R. Durak, E. Öz, K-shell X-ray production cross-sections and fluorescence yields in some medium-Z elements, Radiat. Phys. Chem. 65 (2002) 199–204. https://doi.org/10.1016/S0969-806X(02)00276-1.

[7] R. Durak, S. Erzeneoğlu, Y. Kurucu, Y. Şahin, Measurement of photon-induced K X-ray production cross-sections for some elements with $40 \leq Z \leq 70$ at 122 keV, Radiat. Phys. Chem. 51 (1998) 45–48. https://doi.org/10.1016/S0969-806X(97)00088-1.

[8] R. Durak, Y. Şahin, Measurement of [Formula Presented]-shell fluorescence yields of selected elements from Cs to Pb using radioisotope x-ray fluorescence, Phys. Rev. A - At. Mol. Opt. Phys. 57 (1998) 2578–2582. https://doi.org/10.1103/PhysRevA.57.2578.

[9] A. Küçükönder, Ö. Söğüt, E. Büyükkasap, E. Küçükönder, H. Çam, Kβ/Kα x-ray intensity ratios for bromine and iodine compounds, X-Ray Spectrom. 32 (2003) 60–63. https://doi.org/10.1002/xrs.620.

[10] U. Cevik, S. Kaya, B. Ertugral, H. Baltas, S.M. Karabidak, K-shell X-ray fluorescence cross-sections and intensity ratios for some pure metals at 59.5 and 123.6 keV, Nucl. Instruments Methods Phys. Res. Sect. B Beam Interact. with Mater. Atoms. 262 (2007) 165–170. https://doi.org/10.1016/j.nimb.2007.06.007.

[11] R. Yilmaz, Kβ/Kα X-ray intensity ratios for Cr, Mn, Fe, and Co excited by 8.735 keV energy, Acta Phys. Pol. A. 133 (2018) 1227–1230. https://doi.org/10.12693/APhysPolA.133.1227.

[12] R. Yılmaz, K β / K α X-ray intensity ratios for some elements in the atomic number range $28 \leq Z \leq 39$ at 16.896 keV , J. Radiat. Res. Appl. Sci. 10 (2017) 172–

177. https://doi.org/10.1016/j.jrras.2017.04.003.

[13] B.H. Alias, Using the Solution Of Schrodinger and Dirac Equation to Calculate Variationally Optimized effective Potentials, Universiy of Baghdad, 1996.

[14] B.A. Shadwick, J.D. Talman, M.R. Norman, A program to compute variationally optimized relativistic atomic potentials, Comput. Phys. Commun. 54 (1989) 95–102. https://doi.org/10.1016/0010-4655(89)90035-0.

[15] M.K. Ramaswamy, On the Z-dependence of Kα 1/Kβ 1 X-ray intensity ratio., in: 2nd Int. Conf. Inn. Shell Ioniz. Phenom., Freiburg, F.R. Germany, 1976: pp. 218–219.

[16] A.C. Thompson, D.T. Attwood, M. Eric, M.R. Howells, J.B. Kortright, A.L. Robinson, J.H. Underwood, K. Kim, J. Kirz, G.P. Williams, J.H. Scofield, A.C. Thompson, D. Vaughan, X-ray data booklet, Second edi, Lawrence Berkeley National Laborator, Berkeley, 2001.

[17] C.M. Lederer, J.M. Hollander, I. Perlman, Table of Isotopes, Sixth Edit, John Wiley and Sons, New York, 1967.

[18] L. Visscher, K.G. Dyall, Dirac-fock atomic electronic structure calculations using different nuclear charge distributions, At. Data Nucl. Data Tables. 67 (1997) 207–224. https://doi.org/10.1006/adnd.1997.0751.